JOURNAL OF MAGNETIC RESONANCE **130,** 45–50 (1998)
ARTICLE NO. MN971272

2D Deuteron Exchange NMR and Stimulated Echoes: Molecular Dynamics of the Vacancy Diffusion in Polycrystalline Benzene

Olaf Isfort, Burkhard Geil, and Franz Fujara

Fachbereich Physik, Universität Dortmund, 44221 Dortmund, Germany

Received January 23, 1997; revised September 3, 1997

Since in crystalline benzene the unit cell consists of four differently oriented molecules, the vacancy diffusion is expected to go along with a corresponding molecular reorientation. Therefore, ^{2}H NMR is able to yield detailed information about the time scale and local geometry of this jump diffusion process. We have carried out ^{2}H NMR stimulated echo and 2D experiments. These data, their fit to calculated spectra, and a comparison between the (1D) stimulated echo treatment and the 2D analysis are presented.

INTRODUCTION

Multidimensional exchange NMR (*1*) has become an established tool for the investigation of molecular dynamics in polymer materials (*2*). Here we report on the application of the 2D exchange experiment to study the vacancy diffusion in a molecular crystal, namely polycrystalline benzene. Additionally we carried out the NMR stimulated echo as a one-dimensional time domain experiment. Since there are far-reaching analogies between the NMR experiment and quasielastic neutron scattering (*3, 4*), these data are processed and interpreted in terms of structure factors. As will be seen, the latter version of the experiment is more suitable for directly obtaining information on the time scale of the dynamic process investigated.

METHODS

The basic principles of deuteron exchange NMR are discussed in detail in the literature (*2, 5–8*). Here we just mention that with two variations of a stimulated echo four-pulse sequence one obtains deuteron NMR signals which are given by

$$F^A(t_1, t_2, t_m) = \langle \sin(\omega_1 t_1)\sin(\omega_2 t_2)\rangle \qquad [1]$$

for the sequence $(\pi/2|_Y - t_1 - \pi/4|_{X-tm} - \pi/4|_X - \Delta - \pi/2|_X - \Delta - t_2)$ and

$$F^Z(t_1, t_2, t_m) = \langle \cos(\omega_1 t_1)\cos(\omega_2 t_2)\rangle \qquad [2]$$

for the sequence $(\pi/2|_Y - t_1 - \pi/2|_Y - t_m - \pi/2|_Y - \Delta - \pi/2|_X - \Delta - t_2)$. In the so-called *preparation period,* before the application of the pulse sequence, the sample builds up an equilibrium magnetization. The first two pulses are separated by the *evolution period* t_1, during which the spins possess the frequency ω_1 relative to the Larmor frequency. During the *mixing period* t_m ($t_m \gg t_1$) the spins change their frequency from ω_1 to ω_2 due to the molecular dynamics under investigation. The NMR signal is recorded within the *detection period* t_2. The fourth pulse is applied as a refocusing pulse in order to circumvent receiver dead time. We used four scan phase cycles to remove unwanted contributions to the signal (*9*). The frequencies ω_1 and ω_2 are determined by the quadrupolar interaction of spin-1 nuclei as given by

$$\omega_{1,2} = \pm \frac{\omega_Q}{2}(3\cos^2\alpha_{1,2} - 1). \qquad [3]$$

α_1 and α_2 are the angles between the principal axis of the nuclear interaction tensor and the external magnetic field before and after the mixing time, respectively. In the systems studied here deuterons are bonded to carbon atoms. Here the principal axis of the interaction tensor is parallel to the molecular bond direction. ω_Q is $\frac{3}{4}$ the quadrupole coupling constant of the deuteron.

In the presence of reorientational dynamics of molecular bonds during the mixing time Eqs. [1] and [2] represent appropriate correlation functions for the investigation of the time scale and local geometry of this dynamic process.

A double Fourier transform of the data sets $F^A(t_1, t_2, t_m)$ and $F^Z(t_1, t_2, t_m)$, keeping t_m constant at a fixed value, leads to a two-dimensional spectrum $S(\omega_1, \omega_2, t_m)$. The details of processing the data to obtain pure absorptive spectra are described in the literature (*2*). $S(\omega_1, \omega_2, t_m)$ is the joint probability density of finding a spin with frequency ω_1 and, by a time interval t_m later, with frequency ω_2. Reorientation of a molecular bond causes a cross peak in the spectrum, the position of which in the (ω_1, ω_2) plane contains information about the reorientation angle β_R, i.e., the local geometry of the dynamic process. In powder samples these cross peaks

1090-7807/98 $25.00

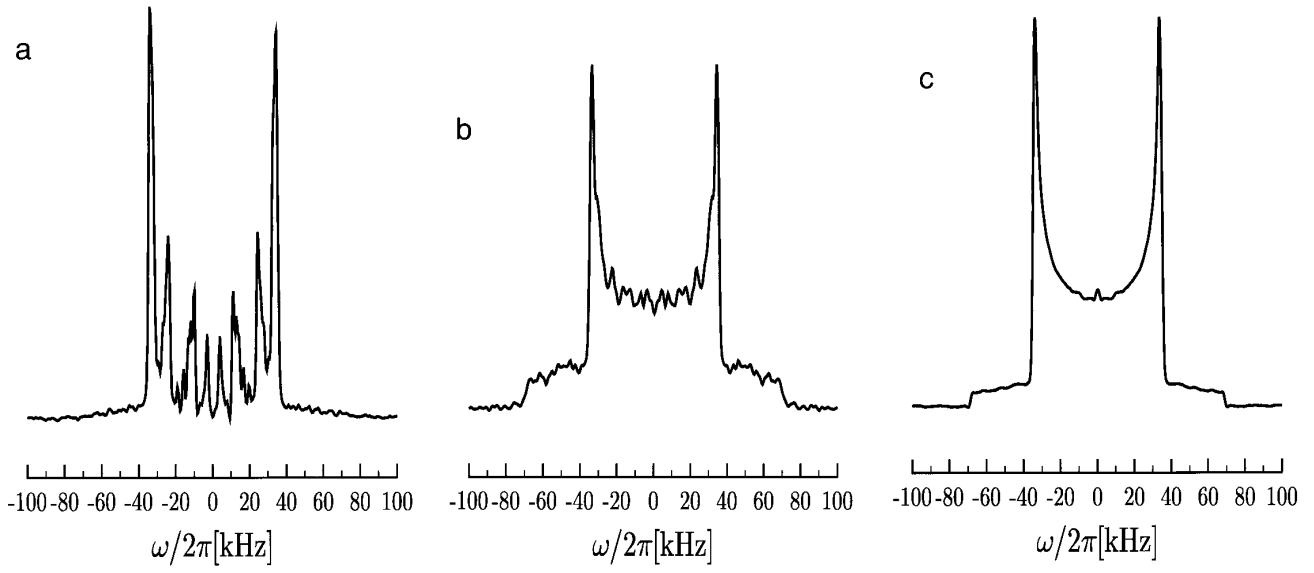

FIG. 1. Solid echo spectra of benzene at 270 K: (a) slowly cooled in the cryostat, (b) rapidly quenched in liquid nitrogen, and (c) benzene in SiO_2 powder, slowly cooled.

occur as singularities forming elliptic features in the spectra. These ellipses can always be found if there is some kind of discrete reorientational jump motion in the sample. In general one observes a distribution of reorientation angles. The resulting 2D spectra are composed of the *subspectra* $S_{\beta_R}(\omega_1, \omega_2)$ which describe reorientational jumps with single reorientation angles β_R. This decomposition can be expressed as

$$S(\omega_1, \omega_2, t_m) = \int_{0^\circ}^{180^\circ} S_{\beta_R}(\omega_1, \omega_2) R(\beta_R, t_m) d\beta_R. \quad [4]$$

$R(\beta_R, t_m)$, the so-called *reorientation angle distribution* (RAD), depends on the mixing time t_m and consequently contains all the information on the time scale and geometry of the dynamic processes under investigation. The subspectra $S_{\beta_R}(\omega_1, \omega_2)$ are independent of time and can be regarded as an experimental filter. An expression can be given for the subspectra:

$$S_{\beta_R}(\omega_1, \omega_2) = \frac{S_0}{\sqrt{6(\omega_1/\omega_Q + 1/2)}\sqrt{6(\omega_2/\omega_Q + 1/2)}} \times \frac{1}{(\sin^2(\beta_R)[1 - \frac{2}{3}(\omega_1/\omega_Q + \frac{1}{2})] - [\pm\sqrt{\frac{2}{3}(\omega_2/\omega_Q + \frac{1}{2})} \pm \cos\beta_R\sqrt{\frac{2}{3}(\omega_1/\omega_Q + 1/2)}]^2)^{1/2}}. \quad [5]$$

One must sum over all sign combinations, and the spectrum is zero if any term under a square root becomes negative.

In the alternative one-dimensional variation of the experiment only the amplitude of the stimulated echo is measured. Thus only one data point at $t_1 = t_2 = \tau$ instead of the whole transient signal is recorded. Thus the measured signal is given by

$$F^A(\tau, t_m) = \langle \sin(\omega_1\tau)\sin(\omega_2\tau)\rangle \quad \text{and}$$
$$F^Z(\tau, t_m) = \langle \cos(\omega_1\tau)\cos(\omega_2\tau)\rangle. \quad [6]$$

The stimulated echo carried out in this way can be regarded as a generalized incoherent scattering experiment (*3, 4, 14*).

If in the stimulated echo experiment the pulse spacing τ is kept fixed while the mixing time t_m is varied, one typically observes an echo decay in two steps. The first decay reveals the loss of correlation due to the molecular dynamics. Here the correlation time τ_c can be directly examined. The echo amplitude decreases until it reaches a plateau value. The additional decay at larger times is caused by spin–lattice relaxation. Neglecting this longitudinal relaxation, one can define the quantity

$$F^{Z/S}(\tau) = \frac{F^{Z/S}(\tau, t_m \to \infty)}{F^{Z/S}(\tau, t_m \to 0)}. \quad [7]$$

In analogy to incoherent neutron scattering $F^{Z/S}(\tau)$ may be called the *elastic incoherent structure factor* (EISF) (*3, 4*). This is the ratio of the plateau value and the initial value of the intermediate scattering function. The τ dependence of the EISF contains detailed information about the local geometry accessible to a particle undergoing the molecular dynamics

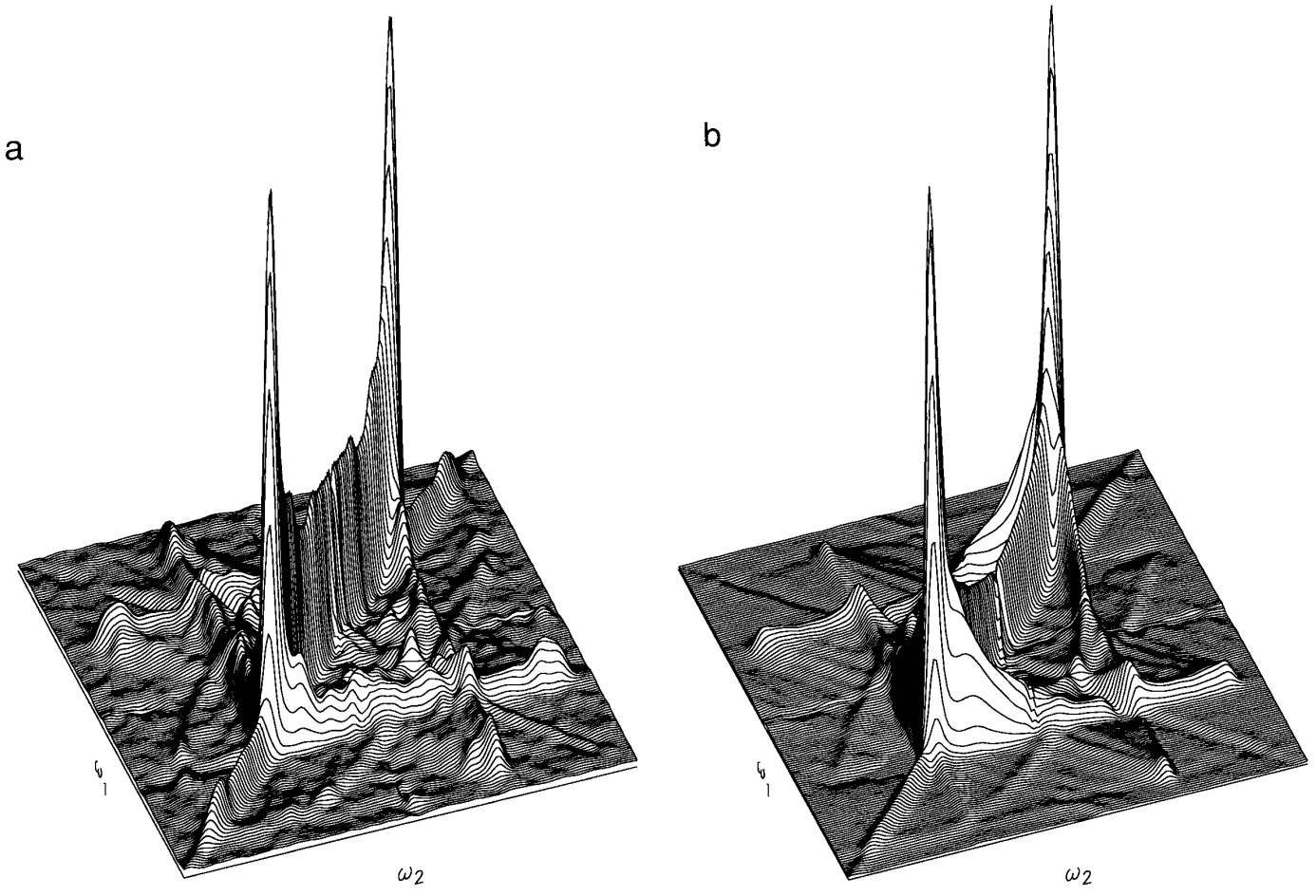

FIG. 2. Experimental 2D spectra of benzene at 270 K, mixing time, 10 ms: (a) quenched benzene sample and (b) SiO_2/benzene sample.

investigated. For N-site jumps the EISF is approximately $1/N$ (with a more detailed τ dependence, see below).

The geometry of the elliptic features in the 2D spectra reflects the value of β_R. This information can also be extracted from the details of the τ dependence in the EISF. While for an N-site jump process the EISF oscillates around $1/N$, this cannot immediately be seen in the 2D spectra. Here a detailed analysis of the cross-peak intensities would be necessary. Another advantage of the 1D treatment is worth mentioning: small angle reorientations are less resolved in 2D spectra due to the prominent diagonal Pake pattern, while the EISF sensitively distinguishes reorientation angles smaller than 10°.

THE SAMPLE

Solid benzene has an orthorhombic crystal structure with a melting point of 278 K. The molecules are located on a stretched fcc lattice. The crystal lattice consists of four sublattices, and the molecular planes of the benzene molecules in each sublattice are differently oriented. The crystal structure has accurately been studied by X-ray (*10, 11*) and neutron diffraction (*12*). Since there are four different molecular orientations in a unit cell, there are three angles between the axes perpendicular to the molecular planes:

$$\angle(\mathrm{I,II}) = 90°, \quad \angle(\mathrm{I,III}) = 27°, \quad \angle(\mathrm{I,IV}) = 84°. \quad [8]$$

On their lattice sites the benzene molecules perform reorientations about their sixfold symmetry axes (*13*). At 270 K, not far below the melting temperature, the correlation time of this motion is of the order of several picoseconds (*14*). In this temperature range one observes motionally narrowed deuteron lineshapes (*15*). The effective principal axis of the nuclear interaction tensor is now perpendicular to the molecular plane.

A much slower reorientational motion in crystalline benzene was detected with proton NMR (*16*). It could be identified as molecular jumps that go along with vacancy diffusion (*17*). A detailed ^{13}C NMR investigation (*18*) in benzene single crystals showed that with the defect diffusion the

molecules perform reorientations between the four different sublattices. Additionally three distinct jump rates were found in these measurements. The conclusion was that jumps between certain lattice planes in the benzene crystal were preferred over jumps within these planes. The ratio of the largest and the smallest jump rates found was between 5 and 10.

The reorientation of benzene in its crystalline state has earlier been used as a model case for the analogy between deuteron NMR stimulated echo and incoherent neutron scattering experiments. The reorientation about the sixfold symmetry axis was investigated with both methods (*14*), yielding consistent results. The defect diffusion in benzene is never fast enough to fall into the dynamic range of neutron scattering, but deuteron NMR stimulated echo measurements in the temperature range not far below the melting temperature have been carried out successfully (*4*). The results—jump rates and activation energies—agree with the aforementioned NMR measurements.

EXPERIMENTAL

The measurements have been performed on a homebuilt NMR spectrometer at a deuteron frequency of 55.3 MHz in an 8.5-T magnetic field (Oxford Instruments, 89-mm RT bore, field inhomogeneity approximately 1 ppm). The signals were recorded in quadrature detection using an eight-bit transient signal recorder. Due to the large width of deuteron spectra (>100 kHz) very short RF pulses are necessary to

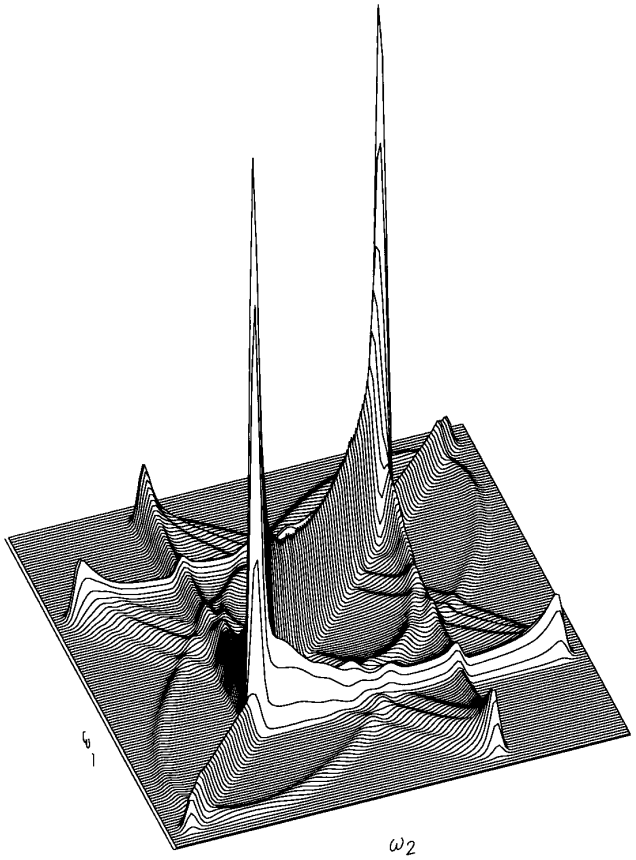

FIG. 3. Theoretical 2D spectrum of benzene, final state ($t_m \gg \tau_c$).

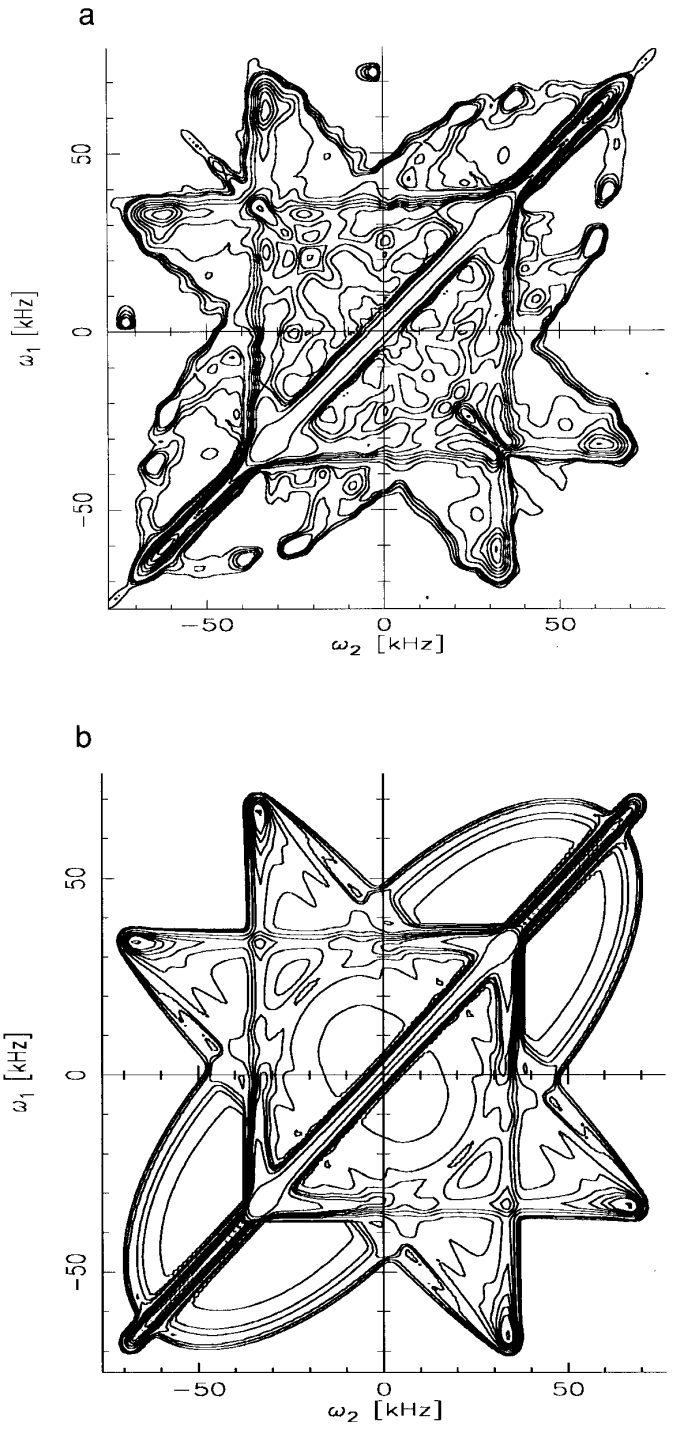

FIG. 4. Contour plots of (a) experimental (quenched sample) and (b) theoretical 2D spectra.

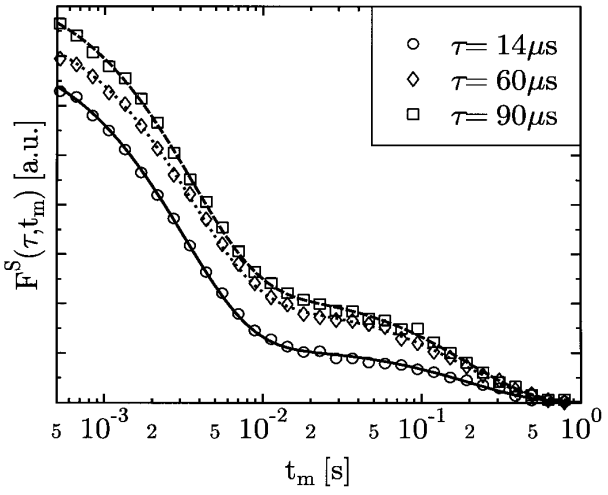

FIG. 5. Stimulated echo decay curves at several evolution times in benzene (quenched sample) at 270 K.

achieve sufficient excitation. Using a 1-kW RF amplifier (ENI) we were able to operate with a $\pi/2$ pulse length of 2.5 μs. The temperature variation of the sample was less than 0.1 K during the measurements (LN_2 Oxford cryostat).

Commercially available benzene-d_6 with an isotopic purity of at least 99.9% served as a sample and was sealed in a Duran glass tube of 4-mm inner diameter and 2-cm length.

RESULTS

At first a solid echo spectrum of the sample is taken (Fig. 1a) at 270 K. Obviously the spectrum obtained does not reveal the expected Pake-like form but a couple of separated (dipolar-broadened) lines. When slowly cooled down from room temperature below the melting point, benzene tends to form single crystals. It is known that benzene tends to orient in magnetic fields (*19*) while in our experiments the deviations of the solid echo spectrum from the powder average are much more pronounced than in the wide line spectra reported in the reference. For our measurements we need a polycrystalline powder while the benzene sample apparently forms a small number of large crystallites instead. A sufficiently good powder average can be obtained by rapidly quenching the sample down from room temperature to 77 K (LN_2) and warming up to 270 K afterward (Fig. 1b). We come to an even better result with benzene in SiO_2 powder with a grain diameter of 5–20 μm (Fig. 1c). The 2D measurements are carried out with samples prepared in the latter two ways. The 1D experiment was performed using the intermediate, rapidly quenched sample.

Figure 2a shows a 2D spectrum of bulk benzene that is obtained at 270 K with a mixing time t_m = 10 ms. Figure 2b shows the same for the SiO_2/benzene dispersion. The off-diagonal intensity in the spectra clearly reveals some reorientational motion on the millisecond time scale. To verify the mechanism of defect diffusion discussed, a theoretical spectrum is calculated using the three reorientation angles in Eq. [8]; see Fig. 3. Contour plots of the experimental and theoretical spectra are given in Fig. 4. The flat elliptical feature that can be found in the spectra corresponds to the reorientation angle of 27°. The other ridges parallel to the frequency axes and orthogonal to the diagonal are caused by the reorientation angles 84° and 90°. Obviously the experimental data agree with the expected motional model of defect diffusion in benzene. Note that even the very closely adjacent 84° and 90° features can be distinguished in the SiO_2/benzene sample (see Fig. 2b).

The 1D stimulated echo experiments are performed as discussed above. The measured data shown in Fig. 5 are examples for the typical correlation decay observed at different values of the evolution time τ. These curves can be well fitted with an initial exponential decay to a plateau value

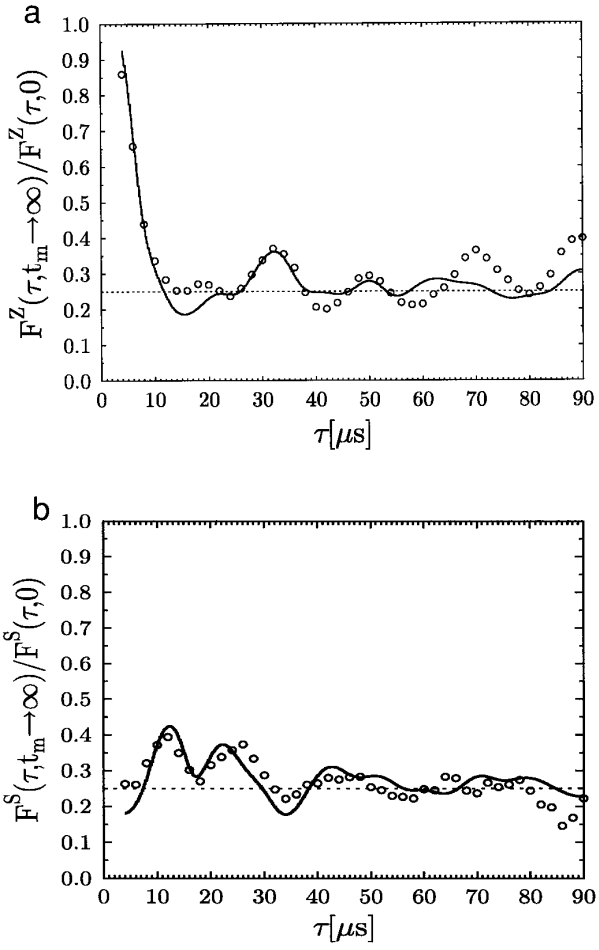

FIG. 6. Experimental and theoretical EISF of crystalline benzene (quenched sample). (a) Cosine part, and (b) sine part.

and a further decay with the spin–lattice relaxation time T_1 or T_{1Q}:

$$F^{Z/S}(\tau, t_m) = (A(\tau)e^{-t_m/\tau_c} + B(\tau))e^{-t_m/T_{1(Q)}}. \quad [9]$$

From these fits one obtains the correlation time τ_c, which is (2.9 ± 0.1) ms at 270 K. The EISF discussed can be calculated as

$$F^{Z/S}(\tau) = \frac{B(\tau)}{A(\tau) + B(\tau)}. \quad [10]$$

The sine and cosine EISF are shown in Fig. 6 as well as the theoretically calculated structure factors. Note that the experimental data directly result from the measurements. No fit parameter is used here. The agreement with the theoretical data is not too bad. The ratio of $\frac{1}{4}$ (four-site jump) can nicely be seen in the experiment. Thus the local geometry of the reorientational dynamics is also verified in the 1D experiment.

Since a measurement at a given evolution time τ has a very high signal-to-noise ratio (see Fig. 5), the visible deviations of the structure factors from the theoretical model are explained with a still disturbed powder average in the benzene sample, though the sample has been treated in the way discussed above. Of course this can already be seen in the solid echo spectra as well as in the 2D spectra: it is always possible to identify sharp spikes in the continuous Pake spectrum. Since the theoretical structure factors are numerically obtained as certain integrals over 2D spectra, the results are quite sensitive on the quality of the powder average.

CONCLUDING REMARKS

Two similar NMR methods for studying slow reorientational molecular dynamics are applied to the case of defect diffusion in a molecular crystal. The advantages and disadvantages of both methods are discussed in comparison.

Two-dimensional exchange NMR spectroscopy is able to determine the translational self-diffusion constant whenever spectral exchange can be assigned to translational motions (*20*). In the case of solid benzene a molecular jump is connected with a reorientation of the quadrupolar interaction tensor. Thus from the knowledge of the lattice constants of crystalline benzene and the correlation time at 270 K one can estimate the diffusion constant:

$$D = \frac{\langle r^2 \rangle}{6t}. \quad [11]$$

$\langle r^2 \rangle$ is the mean square of the distance between nearest neighbors in the crystal and t equals τ_c. This yields $D \simeq 1.8 \times 10^{-17}$ m^2/s.

It is mentioned above that the correlation decays in the 1D experiments are fitted with a single exponential while three different jump rates are reported in the literature (*18*). Actually the single exponential fits work well (see Fig. 5). In the powder experiments discussed here one is not able to distinguish two or more distinct time constants which are of the same order of magnitude. However, in the case of broader correlation time distributions, like in polymers or glasses, nonexponential decays can nicely be seen even in the powder experiments (*21*).

REFERENCES

1. R. R. Ernst, G. Bodenhausen, and A. Wokaun, ''Principles of Nuclear Magnetic Resonance in One and Two Dimensions,'' Clarendon Press, Oxford (1987).
2. K. Schmidt-Rohr and H. W. Spiess, ''Multidimensional Solid-State NMR and Polymers,'' Academic Press, London (1994).
3. F. Fujara, S. Wefing, and H. W. Spiess, *J. Chem. Phys.* **84**(8), 4579 (1986).
4. G. Fleischer and F. Fujara, *in* ''NMR, Basic Principles and Progress'' (P. Diehl, E. Fluck, H. Günther, R. Kosfeld, and J. Seelig, Eds.), Vol. 30, Springer, Berlin (1994).
5. H. W. Spiess, *J. Chem. Phys.* **72**(12), 6755 (1980).
6. S. Wefing and H. W. Spiess, *J. Chem. Phys.* **89**(3), 1219 (1987).
7. S. Wefing, S. Kaufmann, and H. W. Spiess, *J. Chem. Phys.* **89**(3), 1234 (1987).
8. S. Kaufmann, S. Wefing, D. Schaefer, and H. W. Spiess, *J. Chem. Phys.* **93**(1), 197 (1990).
9. D. Schaefer, J. Leisen, and H. W. Spiess, *J. Magn. Reson. A* **115,** 60 (1995).
10. E. G. Cox, *Rev. Mod. Phys.* **30,** 159 (1958).
11. E. G. Cox, D. W. J. Cruickshank, and J. A. S. Smith, *Proc. R. Soc. London Ser. A* **247,** 1 (1958).
12. G. E. Bacon, N. A. Curry, and S. A. Wilson, *Proc. R. Soc. London Ser. A* **279,** 98 (1964).
13. U. Haeberlen and G. Maier, *Z. Naturforsch. A* **22,** 1236 (1967).
14. F. Fujara, W. Petry, W. Schnauss, and H. Sillescu, *J. Chem. Phys.* **89**(4), 1801 (1988).
15. C. P. Slichter, ''Principles of Magnetic Resonance,'' Springer, Berlin (1978).
16. R. Van Steenwinkel, *Z. Naturforsch. A* **24,** 1526 (1969).
17. D. E. O'Reilly and E. M. Peterson, *J. Chem. Phys.* **36**(11), 5536 (1972).
18. T. Gullion and M. S. Conradi, *Phys. Rev. B* **32**(11), 7076 (1985).
19. R. Hentschel, J. Schlitter, H. Sillescu, and H. W. Spiess, *J. Chem. Phys.* **68,** 56 (1978).
20. J. J. Titman, Z. Luz, and H. W. Spiess, *J. Am. Chem. Soc.* **114,** 3757 (1992).
21. F. Fujara, B. Geil, H. Sillescu, and G. Fleischer, *Z. Phys. B: Condens. Matter* **88,** 195 (1992).